Contrib Mineral Petrol (2007) 153:405–416
DOI 10.1007/s00410-006-0154-8

ORIGINAL PAPER

Textural evolution of polyhedral olivine experiencing rapid cooling rates

François Faure · Pierre Schiano · Gilles Trolliard · Christian Nicollet · Bernard Soulestin

Received: 7 February 2006 / Accepted: 23 October 2006 / Published online: 15 November 2006

Abstract Dynamic crystallization experiments in the $CaO–MgO–Al_2O_3–SiO_2$ (CMAS) system have been used to investigate the change in crystal shape when pre-existing polyhedral olivine crystals are cooled rapidly (1,639–2,182°C/h). Polyhedral olivines are crystallized initially in a first step using a slow cooling rate (2°C/h), then skeletal and dendritic overgrowths develop on the polyhedral crystals during a subsequent fast cooling event. During this second episode small dendritic olivines also nucleate within the liquid phase. Observation of the experimental sample by optical microscopy shows that the polyhedral olivine shape progressively changes to a skeletal and then to a dendritic morphology in the following sequence: polyhedral ⇒ hopper polyhedral ⇒ dendritic polyhedral. This evolutional sequence is discussed in terms of changes in the crystal growth conditions during cooling and a general relation between these olivine dynamic crystallization experiments and the integrated model of crystal growth by Sunagawa (Bull Minér 104:81–87, 1981, Morphology of crystals, Terra Scientific Publishing Company, 1987) is proposed.

Communicated by J. Hoefs.

F. Faure (✉)
Centre de Recherche Pétrographiques et Géochimiques, CNRS-UPR2300, 15 rue Notre Dame des Pauvres, BP 20, 54501 Vandoeuvre les Nancy, France
e-mail: ffaure@crpg.cnrs-nancy.fr

P. Schiano · C. Nicollet
Laboratoire Magmas et Volcans, OPGC-Université Blaise Pascal-CNRS, 5 rue Kessler, 63038 Clermont-Ferrand, France

G. Trolliard · B. Soulestin
Science des Procédés Céramiques et de Traitements de Surface, UMR 6638 CNRS, 123 avenue Albert Thomas, 87060 Limoges Cedex, France

Introduction

Deciphering the thermal history of magmas prior to eruption is necessary to fully understand volcanic processes. Numerous magmatic processes can occur, such as magma mixing, convection and differentiation in the magma chamber. They represent important events governing the rates and mechanisms of the crystallization process of mineral species within the magma. The in-depth investigation of magmatic paragenesis is thus one of the main tools to shed light upon the processes prevailing during the early thermal history. There are several ways to investigate the generally complex thermal history of magmas.

A traditional method requires the use of chemical variations in minerals, such as zoning patterns, which result from the evolution of both chemical and physical conditions during the solidification of magma. For example, zoned plagioclase feldspars, as members of a continuous reaction series, have marked sensitivities both to the variations of the parameters in the P-T crystallization path and to the evolution of the bulk composition of crystallizing melts (Stamatelopoulou-Seymour et al. 1990; Singer et al. 1995; Devine et al. 1998; Zellmer et al. 1999). Olivine is also able to crystallize over an extended temperature range and thus the change in composition of this mineral could also reflect the evolution of external physico-chemical processes (Miyamoto et al. 1986; Nakagawa et al. 2002;

Pan and Batiza 2002; Morgan et al. 2004). However, chemical zoning in olivine is seldom seen, as interdiffusion between iron and magnesium is efficient enough to obliterate the compositional zoning characteristic of these growth conditions (Chakraborty 1997).

An alternative method is to study reaction textures in volcanic rocks. However, reaction rims are generally very narrow (Ingrin and Poirier 1986; Faure et al. 2001) and transmission electron microscopy (TEM) is generally required. This technique can be a powerful tool to assess significant structural features of the pre-eruptive setting of magmas, but owing to the difficulties linked to sample preparation the application is often limited.

Finally, it has been shown that the morphologies of nascent crystals, as well as their final shape, are determined both by thermodynamic and kinetic criteria so that the crystal habit directly reflects the geological conditions prevailing during its formation (Faure and Schiano 2004). Conversely, changes either in P, T conditions or cooling rate occurring within silicate melts can be logically investigated by observation of crystal habits (e.g., Donaldson 1982; Faure et al. 2003a). Generally crystal habit can be characterized by optical microscopy of a thin section. These typical magmatic microstructures are often well preserved, even during subsequent metamorphic events, so long as the rocks do not suffer intense strain. This property is particularly useful for studying old lavas such as komatiite rocks (Pyke et al. 1973; Donaldson 1982; Arndt 1994).

Olivine is a common mineral of basaltic magmas. The influence of the degree of undercooling and cooling rate on the crystalline morphology of olivine was first studied by Donaldson (1976), who detailed ten categories of olivine shape related to increasing cooling rate and/or degree of undercooling but did not propose a developmental model to explore the relationship between these morphologies and crystal growth mechanisms.

Based on the assumption that natural crystallization in magmas can be viewed as a crystal growth process taking place from a high temperature solution, Sunagawa (1981, 1987) has proposed an integrated model in which he combines habit changes, single face crystal growth rates, and growth mechanisms as a function of the supersaturation (or degree of undercooling) in a unique diagram. This integrated model suggests the variation of crystal morphology depends mainly on the degree of supersaturation of the solution. Kirkpatrick et al. (1981) have applied the same approach to understand the shape of olivine crystals. This attempt has been particularly successful to account for a few specific olivine habits, principally the so-called skeletal habit as described by Faure et al. (2003a), but most of the ten crystal shapes presented by Donaldson (1976) remain unexplained.

Recently, based on forsterite dynamic crystallization experiments combined with SEM and TEM observations, Faure et al. (2003a, b) have restricted to three the number of shapes that rapid-growth olivines can adopt with increasing degrees of undercooling: tabular, hopper (skeletal) and swallowtail (dendritic) morphologies. They propose that other forsterite shapes previously described in the literature correspond, in fact, to particular sections of these three shapes. The influence of the synthesis parameters, degree of undercooling versus cooling rate, on the transition between tabular, hopper shape and dendritic growth has been previously investigated (Faure et al. 2003a), but up to now the behavior of slow cooled polyhedral olivine crystals submitted subsequently to high cooling rates was unknown. The purpose of this contribution is to investigate experimentally the morphological evolution of polyhedral olivine crystals experiencing subsequent episodes of high cooling rate, i.e., the evolution of such crystals in a magma partially crystallizing and then erupting. These results enhance knowledge of the change in olivine habit as a function of physical synthesis parameters, and allow us to analyze and subsequently discuss the relationship between olivine shapes and crystal growth mechanisms.

Experimental procedures

The experimental techniques used in this study have been described previously in Faure et al. (2003a). Experiments were carried out in the CaO–MgO–Al_2O_3–SiO_2 (CMAS) model system at 1 atm., except for two experiments (DP-521 and DP-518) which were contaminated by sodium during the steps of cooling. The two experiments were instead performed in the CaO–MgO–Al_2O_3–SiO_2–Na_2O (CMASN) system. The starting glass material was prepared from a mixture of reagent grade oxides (51.34 wt% SiO_2, 14.14 wt% Al_2O_3, 17.39 wt% CaO and, 17.11 wt% MgO), melted in a platinum capsule at 1,400°C (i.e., about 50°C above the liquidus temperature: T_{liq} = 1,342°C) for 24 h in air, and quenched into water. The obtained glass was ground in an agate mortar and the resulting powder was formed into a 3–4 mm pellet, placed on a platinum wire loop (Donaldson et al. 1975a) and fused in a 1 atm. vertical furnace. Temperature was measured using a PtRh6/PtRh30 thermocouple, located within 1 cm of the pellets and calibrated against the

melting points of gold (1,064°C) and palladium (1,552°C).

The charges were first melted for 1 h above the liquidus (22°C < + ΔT < 52°C), +ΔT: the degree of superheating corresponding to the difference between the annealing temperature and the liquidus temperature at start (Fig. 1; Table 1). Then, the charges underwent a step of low cooling rate (2°C/h: see the bold line A in Fig. 1) in order to crystallize polyhedral crystals, with a subsequent high cooling rate episode to develop dendritic overgrowths on the polyhedral crystals. For this, variable high cooling rates were adopted (1,639–2,182°C/h: see the fine lines B and C in Fig. 1), beginning at temperatures Tc. At the end of the experiments, the charges were quenched by dropping them into water (dashed lines in Fig. 1).

Two parameters related to temperature differences can be defined for these experiments: Td (the temperature of differentiation) is the difference between the liquidus temperature and the temperature at the end of the slow cooling step, and $-\Delta T_n$ (nominal degree of undercooling) corresponds to the difference between this final temperature and the quenching temperature (Fig. 1). Note that Td gives the temperature interval during which most of the crystallization occurs, i.e., the formation of polyhedral olivine. Consequently, the crystallization rate increases with increasing Td values. As the composition of the residual liquid surrounding the crystallites is directly relevant to the proportion of crystallites formed, the variation of Td is thus a key factor in varying the chemical composition of the liquid in which the dendrites grow during the subsequent high cooling rate episode. The equilibrium liquid line of differentiation of the system, corresponding to the equilibrium liquid at the end of the slow cooling step (Tc), has been determined in a previous study (Fig. 2; Table 2 in Faure and Schiano 2005) by analyzing the host glass of the charges at a distance >100 μm around the crystals formed during the second step of rapid cooling; i.e., in a zone unaffected by their growth.

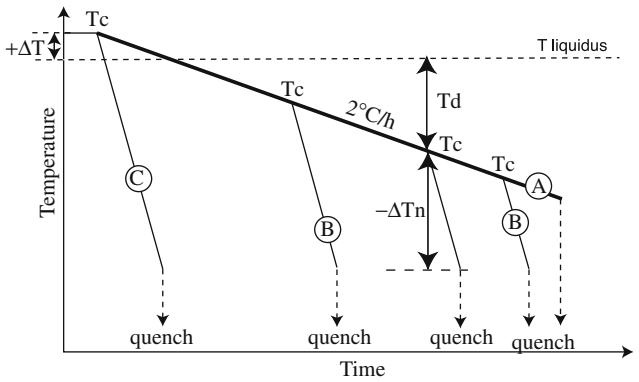

Fig. 1 Schematic diagrams showing the three experimental protocols used in the study. *A* Dynamic crystallization experiments at low cooling-rates to crystallize polyhedral olivine, *B* complex dynamic crystallization experiments to crystallize dendritic polyhedral olivine. An initially low cooling-rate step creates the polyhedral shape and a subsequent high cooling-rate step produces the skeletal or dendritic overgrowths. *C* Dynamic crystallization experiments at high-cooling rates to crystallize skeletal or dendritic olivine as a function of the quench temperature. Td corresponds to the difference between the liquidus temperature and the temperature at the end of the slow cooling step, and –ΔTn corresponds to the difference between the temperatures at the final slow cooling step and the quenching temperature. Tc is the temperature at the beginning of the high cooling-rate step

The adopted protocol reproduces the crystallization scheme of magma in the crust experiencing an initial low cooling rate during which the crystallization begins, followed by a subsequent high cooling rate step during eruption at the surface. Such examples are common events in nature as they represent the majority of magmas that are not superheated at the time of eruption. A similar experimental protocol (with, however, a restricted range of temperature of differentiation) was used by Donaldson et al. (1975b) to estimate the conditions of crystallization of lunar basalts.

After the experiments, the charges were mounted in epoxy and prepared as doubly polished thick or thin sections. The sections were studied by optical and scanning electron microscope (SEM). SEM work was carried out at the Université Blaise Pascal (Centre Régional de Mesure Physique, Clermont-Ferrand) on a JEOL 5910LV equipped with an X-ray analyzer PGT operating in energy-dispersive mode (EDS). We used mainly the backscattered electron mode on polished thin sections, with 15 kV accelerating voltage, 2 nA probe current and 19 mm working distance. Compositions of glasses were determined by electron microprobe analyses on a Cameca SX100 at the Université Blaise Pascal (Centre Régional de Mesure Physique, Clermont-Ferrand). Beam conditions of 15 kV and 10 nA were employed and the electron beam was focused. However, for analyses of glass in the CMASN experiments, the beam was spread to 5 μm diameter to minimize alkali migration.

Results

All charges contain large polyhedral forsterite crystals, ranging from a hundred microns to a few millimeters, produced during the slow cooling event. These crystals always coexist with very small crystals (<100 μm)

Table 1 Results of experiments

Run no.	+ΔT (°C)	d(Td)/dt (°C/h)	Td	d(–ΔTn)/dt (°C/h)	–ΔTn (°C)	Size of dendrite ST (μm)	Size of dendrite DP (μm)	Dendrite growth rate (ST) (10^{-8} m/s)	Dendrite growth rate (DP) (10^{-8} m/s)
DP-573	40	2	24	1,644	236	170	140	32.8	27.0
DP-576	38	2	42	1,730	208	100	105	23.1	24.2
DP-422	52	2	50		210	75	65		
DP-577[a]	38	2	74	1,652	186	25	30	6.1	7.4
DP-578[a]	38	2	80	1,639	175	27.5	25	7.1	6.5
F2/545[a]	22	2	116			0	0	0	0
F2/507	46	1,890	216	1,890		280		82.6	
F2/506	46	1,890	242	1,890		340		60.7	
DP-521[b]	41	2	108	2,182	140	20	20	8.6	8.6
DP-518[b]	43	2	70	1,782	70	125	125	88.3	88.3

$+\Delta T = T_{initial} - T_{liquidus}$, $Td = T_{liquidus} - T_{end\ of\ the\ slow\ cooling\ step}$, $-\Delta Tn = T_{end\ of\ the\ slow\ cooling\ step} - T_{quench}$, *ST* swallowtail morphology, *DP* dendritic polyhedral

[a] Clinopyroxene has been observed in the charge

[b] Correspond to charges that display Na in their residual glass

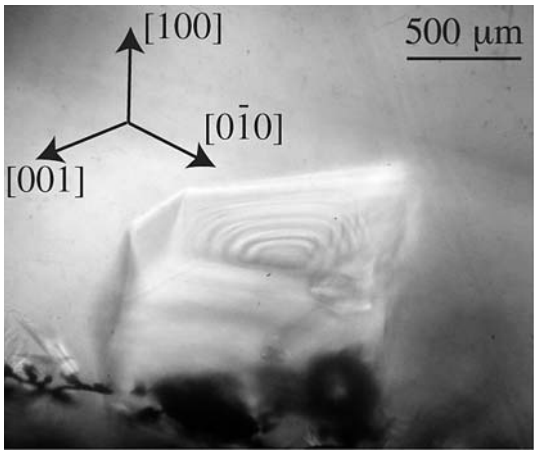

Fig. 2 Photomicrograph of a hopper polyhedral crystal displaying one of the two large cavities that replace the (100) faces, (cooling rate 1:2°C/h, Td = 80°C, cooling rate 2:1,639°C/h, –ΔTn = 175°C)

produced during the rapid cooling stage of the experiments. This rapid cooling event induced transformations in the polyhedral crystals, which will be described below.

Location of crystals in the experimental charges

Large polyhedral crystals are always located on the border of the bead. They generally appear to have nucleated on the platinum wire, or on air bubbles trapped during the sample preparation. In contrast, small micro-crystals are found both on the border of the charge where they radiate from the platinum wire, and within the charge. These two crystal habits represent two generations of crystals resulting from two successive nucleation events. The formation of a small number of polyhedral crystals is achieved over a long period of time (12–54 h), whereas the second generation gives rise to a large number of micro-crystals in less than 10 min. Small dendritic clinopyroxenes are also present in three charges corresponding to the more differentiated liquids (Table 1). Below, we first describe the evolution of the large, polyhedral crystals when they are submitted to high cooling rates, and then consider the evolution of the small micro-crystals.

Table 2 Chemical composition of glass located at a distance >100 μm around the dendritic and skeletal crystals formed during the second step of rapid cooling present as host glasses in experiments

Sample	F2/219	DP-573	DP-576	DP-422	DP-577	DP-578	DP-545[a]	DP-518	DP-521
Td (°C)	0	24	42	50	74	80	116	70	108
Temperature (°C)	1,342	1,318	1,300	1,292	1,268	1,262	1,226	1,272	1,234
SiO_2	51.61	51.35	51.53	51.70	51.61	51.84	54.39	48.79	49.84
Al_2O_3	14.33	14.93	15.30	15.58	15.87	15.97	17.50	14.97	15.60
MgO	16.63	15.26	14.40	13.87	12.85	12.57	10.12	11.77	10.53
CaO	17.41	18.43	18.74	18.82	19.65	19.60	17.96	18.27	19.21
Na_2O								6.16	4.80

[a] Analyzes were performed in glass inclusions located in polyhedral olivines

Evolution of polyhedral shaped crystals during high cooling rates

Evolution of the polyhedral morphology of olivine crystals experiencing a high cooling rate episode can be divided into two steps.

Polyhedral crystal → hopper polyhedral crystal (or skeletal crystal)

Figure 2 shows prismatic crystal very characteristic of the crystal habit of olivine described in the literature (Deer et al. 1962). This polyhedral crystal has evolved towards the formation of a hopper form, as shown by the development of a large cavity at the top of the crystal. Thus, in hopper polyhedral crystals, (100) faces are never observed and each extremity of the hopper crystal is ended by one such large cavity, which is filled with liquid, now quenched to glass. The general shape of the cavities is more or less hexagonal and their internal diameters decrease from the crystal surface to the apex inside the crystal. The internal morphology of the cavities thus resolves into a stair-like structure formed by macro-steps (Fig. 2). Such hollows are typical features of the skeletal forsterite morphology (Donaldson 1976; Sunagawa 1987; Faure et al. 2003a). When observed in a section almost parallel to the (100) plane, hopper polyhedral crystals seem to contain elongated glass inclusions parallel to the (010) and (021) faces of the crystals (Fig. 3). In fact, the glass inclusions are open (i.e., connected with the external liquid) and reflect the liquid that becomes trapped at the pit of each of the macro-steps. These ''open inclusions'' are formed during formation of the stair-like texture and are thus associated with the late rapid-cooling stage of the experiments.

Hopper polyhedral crystal → dendritic polyhedral crystal

Dendritic polyhedral morphology was previously described as polyhedral habit with additional dendritic overgrowths on the corners by Kirkpatrick et al. (1981) and Faure et al. (2001). Similar microstructural features are observed in our experimental charges (Fig. 4). However, nascent dendritic overgrowths can also be found inside the hopper polyhedral cavities, where they develop on the pit of the steps. Figure 5 shows that several generations of branches compose the dendrites. Numerous dendritic arms appear simultaneously in the cavities and constitute the first order. The second order of branches develops on the primary ones and a third generation is also visible by slight focus adjustment of the optical microscope.

Figure 6 shows SEM observations carried out on an experimental charge in which euhedral olivine crystals (dark contrast) are surrounded by the glass (bright contrast). Within the glass are numerous dendritic rods. In the general overview (Fig. 6a) they generally exhibit random orientation. However, detailed examination shows that around a particular olivine crystal (labeled A), rods are parallel (see arrows in Fig. 6a) and the two (010) faces of the polyhedral crystal (see arrows in Fig. 6b) have the same orientation as these parallel rods. This suggests that the host polyhedral crystal controls the rod formation, although no connection is observed in this section plane between rods and polyhedral olivine. To test this interpretation, the section was made thinner. Figure 6c is a backscattered SEM image obtained after sample thinning; rods are still present and extend closer to the polyhedral olivine

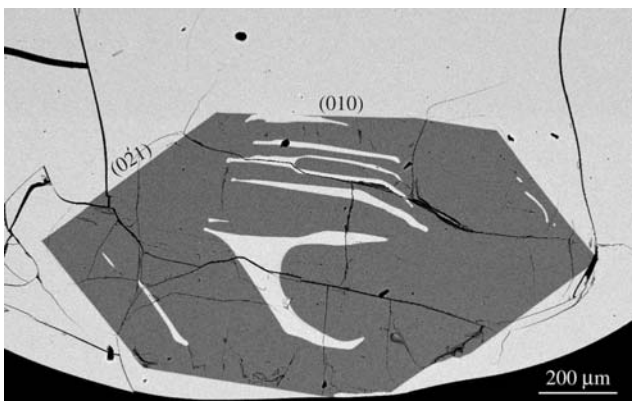

Fig. 3 Backscattered electron photo of a section almost parallel to (100) plane inside a skeletal polyhedral olivine, (cooling rate 1:2°C/h, Td = 80°C, cooling rate 2:1,639°C/h, –ΔTn = 175°C)

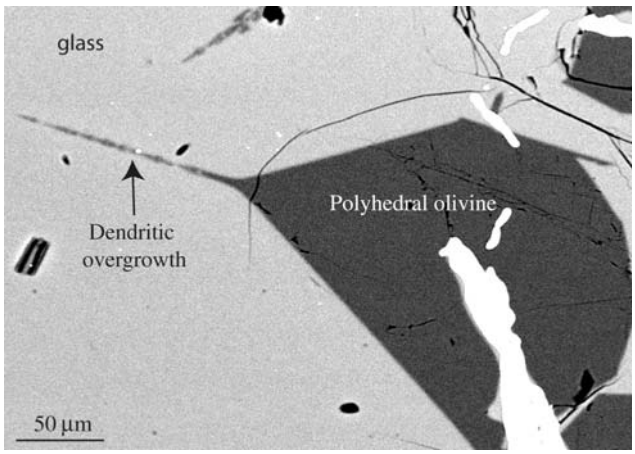

Fig. 4 Backscattered electron photo showing a polyhedral olivine with a dendritic overgrowth on a corner, (cooling rate 1:2°C/h, Td = 24°C, cooling rate 2:1,644°C/h, –ΔTn = 236°C)

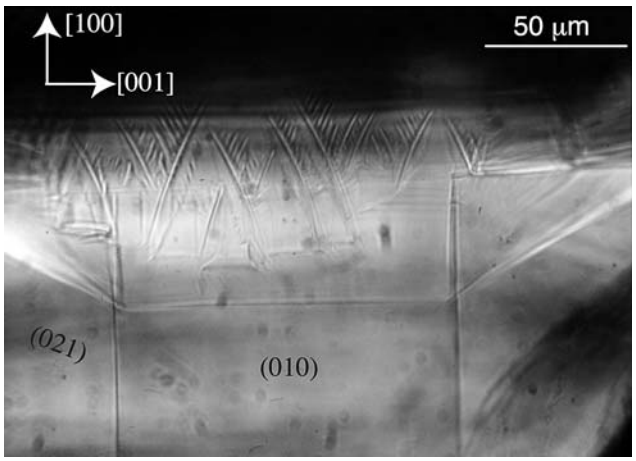

Fig. 5 Photomicrograph showing dendritic fibers inside the cavity of a hopper polyhedral olivine, (cooling rate 1:2°C/h, Td = 70°C, cooling rate 2:1,782°C/h, –ΔTn = 70°C)

crystal. Figure 6d shows a schematic representation of the locations of rods in the two cross sections (Fig. 6b, c). The common crystallographic orientation for rods and olivine polyhedral crystals was also established by observations in optical microscopy performed between crossed polars; This type of set of parallel rods always reveal a straight extinction and extinguish simultaneously with their host polyhedral olivine crystal on which they grow. All these observations suggest that this rod microstructure corresponds to the formation of dendrites on polyhedral crystals. The inner microstructure of rods shown in Fig. 6c is very like that observed in low magnification TEM images obtained on sections of the (010) dendritic lamellae (Faure et al. 2003b). In the two cases, rods correspond to cross-sections of (010) dendritic lamellae and are formed by the juxtaposition of structural units showing dove-shaped morphology. Therefore the observed microstructure is very similar to that of dendrites produced during conventional dynamic crystallization experiments (i.e., without a first low-cooling rate step; Faure et al. 2003b). The sets of parallel rods account for the different generations of arms involved in the formation of a dendrite.

Finally, it is important to note that the number of rods growing on olivine crystals differs, depending on

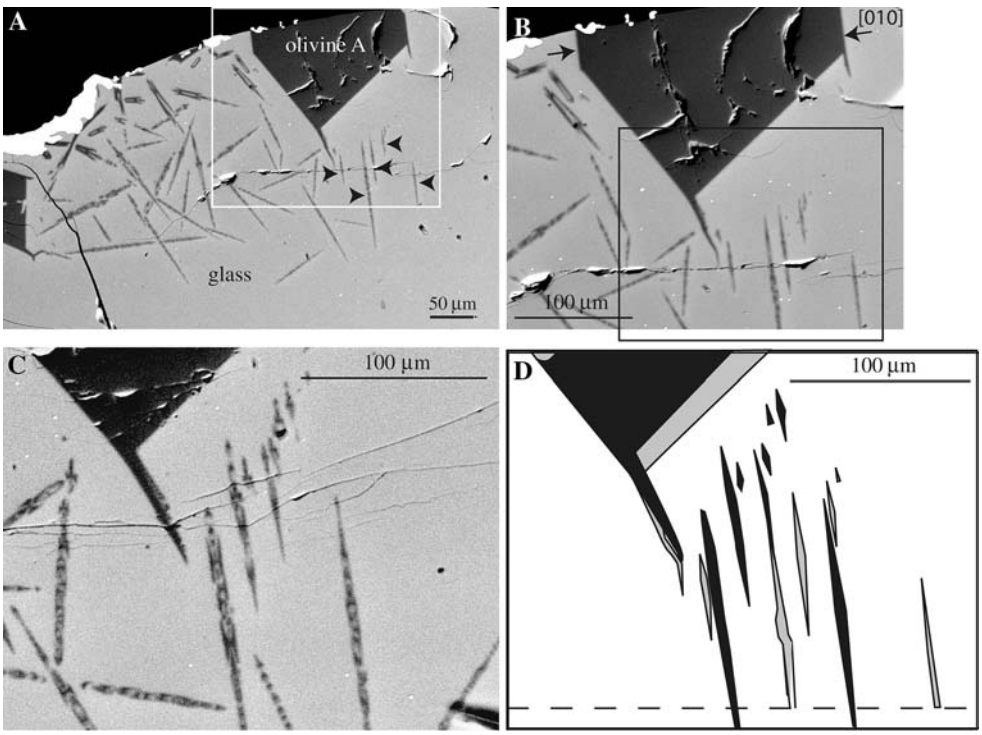

Fig. 6 Backscattered electron images displaying sections at different depths in a dendritic polyhedral forsterite, (cooling rate 1:2°C/h, Td = 24°C, cooling rate 2:1,644°C/h, –ΔTn = 236°C). **a** Overview showing both dendritic rods associated to polyhedral olivine and randomly orientated dendritic rods corresponding to micro-crystals. The box locates the area displayed in **b**. **b** Enlargement of the rectangular area in **a**, showing two faces of the polyhedral crystal (*arrows*) that have the same direction to the elongated rods. **c** Enlargement of the rectangular area in **b** but at a deeper level of sectioning. New dendritic parallel rods are visible inside the cavity of the dendritic polyhedral olivine. **d** Sketch showing superimposition of dendritic polyhedral crystal at various depths of sectioning. Areas in *grey* are related to box photo **b** and *black* areas correspond to section photo **c**

the depth of the crosscutting section of the crystal. However, as a general rule, for a given crystal the number of rods is always higher in the case of dendritic polyhedral crystals (Fig. 6b–d) than for swallowtail olivine (see Faure et al. 2003a).

Evolution of the micro-crystals during high cooling rates

Micrometer sized olivine crystals found in the charges always have a dendritic morphology. In a section parallel to the (010) plane they display a swallowtail shape (Fig. 7), which represents the final stage of evolution of olivine morphology as a function of the degree of undercooling (Faure et al. 2003a). In fact the center of the swallowtail morphology is constituted by a small micro-crystal that presents a hopper type morphology, i.e., an hourglass shape on which dendritic overgrowths have subsequently developed. In our charges, the v-shaped hopper cavities observed in the center of the swallowtail shape indicate that this morphology does not derive from an evolution of a previous tabular crystal but rather directly nucleates in the range of occurrence of the hopper habit (Faure et al. 2003a). The size of swallowtail crystals is highly variable in the same charge. This suggests a continuous nucleation event during the second step of rapid cooling. Whatever the size of the swallowtail crystal, only one dendritic lamella developed on each side of the hourglass shape. This observation is corroborated by other observations in randomly orientated sections in which the absence of parallel rods is characteristic.

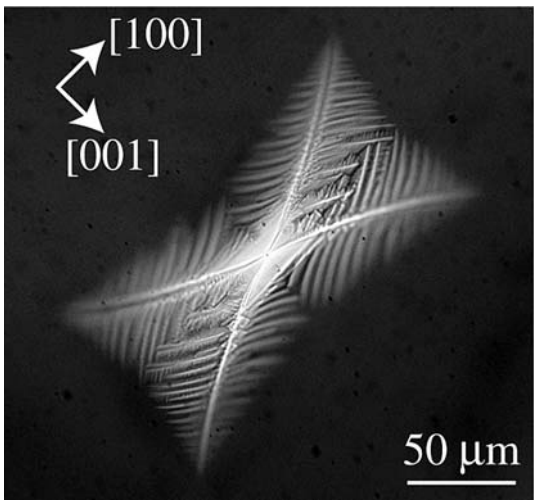

Fig. 7 Photomicrograph of swallowtail olivine observed in a section parallel to the (010) plane, (cooling rate 1:2°C/h, Td = 42°C, cooling rate 2:1,730°C/h, –ΔTn = 208°C)

Dendritic growth rates

Size of the dendrites has been measured both on polyhedral and swallowtail crystals, and the maximum dendritic lengths are reported in Table 1. For micro-crystals, dendrites were measured systematically on crystals orientated parallel to the (010) plane (swallowtail shape). Average dendritic growth rates can then be calculated if several approximations are made, depending on the nature of the crystal used: dendritic polyhedral or swallowtail olivine. For dendritic polyhedral olivine, the time necessary to transform polyhedral crystals into skeletal polyhedral olivines is assumed to be short enough to be ignored. Similarly for the swallowtail morphology, both nucleation delay and time involved in the formation of the skeletal step are supposed to be nil. It is, however, worth noting that the size of the longer dendrites is almost constant within a charge, as well as on hopper polyhedral and swallowtail crystals. This result supports the assumption that the nucleation delay involved in the formation of dendrites on swallowtail crystals can effectively be ignored.

Dendritic growth rates decrease with increasing Td (Table 1). Figure 8 shows the variation of dendritic growth rates as a function of the temperature Tc at the onset of dendritic growth, assuming that nucleation and skeletal step growth can be ignored. Dendritic growth rates as a function of Tc seem well described by an exponential law.

- The upper limit of the dendritic growth rate is obtained for charges directly cooled at a constant, high rate (1,890°C/h), so without the first slow cooling step. The obtained growth rates are probably not accurately determined as the charges are crowded with dendritic olivine crystals, which may collide during crystal growth. Due to crystal closeness, the crystal growth could thus be slowed down, minimizing the determined values of growth rates. However, these experiments can be considered to estimate the minimum size of the longer dendrite and thus the minimum growth rate in the optimal experimental conditions (Td = O).
- The lower limit of the dendritic growth rate could be approached by the interpolation of the trend defined by Fig. 8, and is well described by an exponential law. An interpolation of the trend has been tested by considering data obtained in a classical cooling experiment where the charge only underwent a step of low cooling rate (2°C/h) until high temperature of differentiation Td is attained (Td = 116°C). In this low cooling-rate experiment, olivine crystals only show polyhedral morphologies

without dendritic overgrowths. Beyond this temperature, forsteritic dendrites do not appear but the charge is crowded with dendritic clinopyroxenes. Thus, this experiment allows assessment of the maximum Td beyond which polyhedral dendrite evolution of olivine crystals becomes impossible because pyroxenes occupy all the available space around them.

As previously stated, it is also important to note that the maximum lengths of dendrites for dendritic polyhedral and swallowtail olivine crystals are very similar (i.e., data for the two types of morphology plot along the same curve) for the same experiment. This observation suggests that the delay of nucleation for the first crystallized swallowtail crystal is not significant and that the skeletal growth rates for polyhedral crystals and micro-crystals are similar.

Experiments DP-521 and 518 must be considered separately because they were performed with different starting glass materials. Their residual glass contains 4–6 wt% of Na_2O (Table 2). Note that the growth rate determined in the charges of these two experiments (in particular DP-521; see Fig. 8) is greater than for Na free experiments.

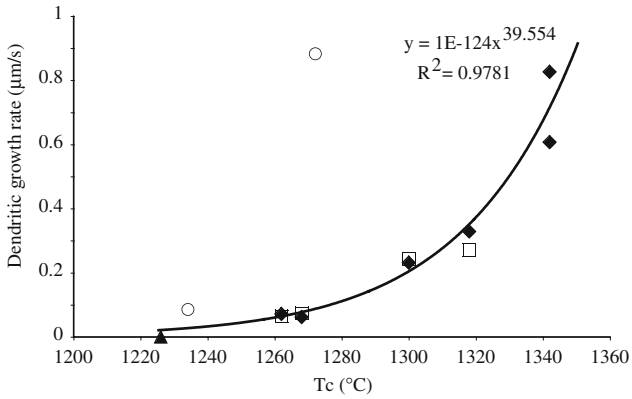

Fig. 8 Dendritic olivine growth rates as a function of Tc (the temperature at the end of the slow cooling step; see Fig. 1). Dendritic growth rate for swallowtail crystals or dendritic polyhedral olivine is similar for a given Tc. *Open square* dendritic growth rate measured for dendritic polyhedral olivine, *black diamond* dendritic growth rate measured for swallowtail olivine, *black triangle* dendritic growth rate measured for polyhedral olivines without dendritic overgrowth (i.e., experiments where the charges underwent only a step of low cooling-rate), *open circles* dendritic growth rate measured for experiments carried out in the CMAS-Na system

Discussion

Influence of chemical and physical parameters on the olivine morphology

These experiments show that small, additional amounts of sodium in the starting material can considerably increase the dendritic growth rate (Fig. 1). Two main hypotheses can be used to explain this result. The addition of Na changes (i) the liquidus temperature and therefore the actual degree of undercooling, and (ii) the physical properties of the liquid, in particular it decreases viscosity which strongly controls crystal growth rate (Baronnet 1984). Nevertheless, the trend of Fig. 8 points out important petrographic implications. It is generally thought that morphologies of olivine crystals in basalts give information on the thermal condition changes during their formation. Accordingly, a polyhedral shape would result from a slow cooling rate while dendrites are generally attributed to rapid cooling events. Olivine morphology is consequently used to obtain information on the cooling conditions of magmas. It is widely assumed that the absence of dendritic features is a key indication that the sample did not experience a rapid cooling episode. Actually, formation of the dendritic morphology also depends on other factors, such as the delay of nucleation and the chemical composition of the magma. Thus, these parameters can induce erroneous conclusions when assessing cooling rates based on the olivine morphology alone. However, the number of rods comprising dendrite overgrowths is very different between hopper and hopper polyhedral crystals. Hopper crystals developed during high cooling rates present narrow cavities and therefore only two dendritic arms can develop, resulting in a swallowtail shape. In contrast, the presence of a large cavity in hopper polyhedral olivine allows growth of several dendrites inside, and thus numerous parallel rods are observable in petrographic sections. Therefore, the presence of numerous parallel rods is indicative of the occurrence of a two stage cooling process of the magma. A major slow cooling event occurs to form polyhedral crystals and a subsequent high cooling rate episode leads to the formation of large hopper cavities and associated dendritic rods.

Evolution of polyhedral morphology as a function of the cooling rate

Charges cooled slowly crystallize polyhedral-shaped olivine even when the nominal degree of undercooling is high (Td = 116°C, see run F2/545). This phenomenon is certainly due to the fact that no actual undercooling exists at the crystal-liquid interface. During

polyhedral crystal growth the crystal faces are in near equilibrium (very low supersaturation) with the host liquid. Consequently no chemical gradient can be observed at the electron microprobe scale in the liquid surrounding a polyhedral crystal (Faure and Schiano 2005). In contrast, polyhedral crystals undergoing a subsequent high cooling rate event display skeletal and then dendritic morphologies. Their morphological evolution is similar to that observed for olivine rapidly cooled in a single stage. Indeed, dynamic crystallization experiments (Faure et al. 2003a) indicate that the morphology of rapid growth olivine evolves from tablet to hopper (skeletal shape) and then to swallowtail (dendritic shape) crystals. In the present new experiments, polyhedral morphology replaces the tablet shape. In addition, these large crystals allow the details of the evolution of the morphology to be distinguished more easily, such as the formation of cavities and the development of dendrites inside.

Formation of polyhedral crystal cavities

Hopper polyhedral crystals show macrostep structures that result from non-uniform supersaturation over the surface of the crystals. This phenomenon, usually called the ''Berg effect'' after Berg (1938), corresponds to an excess of supersaturation at the corners of the crystal, which enhances preferential growth. Growth layers spread inward from the edge thus forming the macrosteps. Crystal growth probably occurs following a 2D nucleation mechanism (VKS mechanism; Volmer 1922; Kossel 1927; Stranski 1928), such as that proposed by Kirkpatrick et al. (1981) for hopper olivine crystallization in conventional dynamic crystallization experiments.

Formation of dendritic polyhedral olivine

Dendrites develop either from crystal corners (Fig. 4) or inside hopper polyhedral cavities (Figs. 5, 6). For the latter location, dendrite formation does not correspond to an optimal condition of growth due to the ''Berg effect'' because it occurs in a zone where the supersaturation is low (Kirkpatrick et al. 1981; Faure and Schiano 2005). This occurrence of overgrowths inside cavities of hopper crystals is also observed in swallowtail crystals formed during a one stage process. It has been interpreted as reflecting a competition mechanism between the growth of dendrites and the growth of the parental hopper crystals (Faure et al. 2003a). Indeed, when dendrite overgrowths nucleate on the corners of hopper crystals, they become trapped inside the cavity of the crystal if the crystal grows faster than the dendrites. Conversely, if the dendrites grow faster than the hopper crystal, growth of the latter is stopped and instead one big dendrite forms at the corners of the crystal. An intermediate situation would involve a similar growth rate for hopper crystals and dendrites. In this case, dendrites oriented towards the center of the cavity would continue to grow during the parent hopper crystal growth.

As the growth velocity of hopper crystals and dendrites is likely to change during cooling, the three configurations mentioned above can be potentially observed in the same charge:

- dendrites only found inside the hopper crystal cavity,
- dendrites developing inside the cavity and propagating outside,
- dendrites occurring only on the corners of the hopper polyhedral crystal.

Transition from polyhedral to dendritic morphology related to crystal growth mechanisms

This part of the discussion deals with crystal growth mechanisms based on the morphological evolution of polyhedral olivine crystals during dynamic crystallization experiments in the model CMAS system. The polyhedral shape of olivine crystals is developed when the degree of undercooling is very small, i.e., at a low cooling rate. In addition, at the scale of the electron microprobe analyses, no compositional gradient is visible at the crystal–liquid interface, indicating that olivine growth is controlled by interface attachment mechanisms (Faure and Schiano 2005). Recent studies have shown that screw dislocation mechanism controls olivine growth when the degree of undercooling (or supersaturation) is low (Cabane et al. 2005). Screw dislocation mechanism is supported by the melt inclusions trapped in polyhedral olivines, which show irregular, usually curvilinear outlines (Faure and Schiano 2005).

On the other hand, if the cooling rate of the crystals is high, the system cannot crystallize olivine fast enough and a high degree of undercooling is reached. Due to the ''Berg effect'' (Berg 1938) higher supersaturation is thus expected near edges than in the center of crystalline faces. This excess of supersaturation at the corners is a favorable situation for preferential growth. Therefore, in order to maintain a constant growth rate of the crystalline faces, the growth mechanism should change and the screw dislocation mechanism should be replaced by the layer-spreading

nucleation (VKS) mechanism. As a consequence, growth layers spread inwards from the corner. They form steps that are distributed in such a way that the decrease of supersaturation at the centre of the surface is compensated by an increase of the step density (Chernov 1974). Macro-steps observed in the cavities of hopper polyhedral olivine (Fig. 2) could be the direct illustration of this change of mechanism. Note that real hopper olivines (i.e., not developed from a parent polyhedral crystal) display similar but smaller macro-steps (Kirkpatrick et al. 1981; Faure et al. 2003a). Thus the change in morphology of polyhedral olivine as a function of the degree of undercooling is in agreement with the integrated model proposed by Sunagawa (1981), in which transition of morphology results from changes in the crystal growth mechanism. Accordingly, the transition between polyhedral and skeletal olivine shapes can be explained by a growth mechanism dominated by dislocations at low degrees of undercooling, and by 2D nucleation when the degree of undercooling increases. Another major difference between polyhedral and skeletal crystallizations is that polyhedral crystallization is controlled by interface attachment mechanisms (probably spiral growth dislocations, see Cabane et al. 2005; Faure and Schiano 2005) whereas skeletal crystallization is diffusion-controlled, even if the growth mechanism is 2D nucleation (VKS). Indeed, chemical profiles performed at olivine skeletal crystal–liquid interfaces display systematic chemical gradients (Faure and Schiano 2005).

At first sight, the transition between skeletal and dendritic morphologies is more difficult to unravel. Indeed, both shapes result from a diffusion-controlled growth. However, according to Sunagawa's model (Sunagawa 1981, 1987), it would be expected that this change in morphology should also result from changes in crystal growth mechanisms. Therefore it seems reasonable to suppose that the skeletal dendritic transition corresponds to a change from 2D nucleation (VKS) to the other diffusion-controlled growth mechanism, i.e., continuous growth. In this case, for atomic species, the establishment of chemical bonds with a growing interface by a continuous mechanism depends on solid–liquid interface roughness. Ideally, almost all surface sites of the crystal can be considered as available kink sites for attachment. As a consequence, for continuous growth, a plot of growth rate-viscosity product versus the degree of undercooling should be a straight line with positive slope passing through the origin (Baronnet 1984). However, to our knowledge, the only available data for dendritic olivine growth rates plot along a line that does not pass through the origin in such a plot (Jambon et al. 1992), thus disagreeing with the continuous growth hypothesis. This is further supported by optical observation of olivine dendrites, which are formed by a succession of units similar to the hopper shape (Faure et al. 2003a) and have a faceted habit that suggests a growth mechanism different from continuous growth. However, TEM investigation at a very local scale of forsterite dendrites indicates that only the external part (≤500 nm) of the dendrite tip displays a non-faceted habit (Fig. 9d in Faure et al. 2003b). This suggests that the final appearance of the dendrites mainly results from textural ripening (Faure et al. 2003b). We thus speculate that accurate, new measurements of dendritic growth rates could be used to evaluate the hypothesis of a continuous growth mechanism for olivine dendrites.

The results are illustrated in Fig. 9, which shows a theoretical plot of the growth rate-viscosity product versus the degree of undercooling and the corresponding development of scenarios for the textural evolution of polyhedral olivine experiencing rapid cooling-rates.

Conclusions

Dynamic crystallization experiments in the CMAS model system suggest that, as proposed by the integrated model of Sunagawa (1981, 1987), variation of olivine morphology could be linked to changes in the growth mechanism. At low degrees of undercooling, a screw dislocation mechanism could control the rate of crystal growth and results in polyhedral-shaped olivine. When the degree of undercooling of the system increases with increasing cooling rate (or a delay of nucleation), crystal growth rate, at least for some faces, would also increase to compensate the resulting supersaturation. Therefore the crystal would follow a surface nucleation growth mechanism, accentuated by the cavities displaying a stair-like texture. It is important to note that although the growth mechanism has changed between polyhedral and hopper (skeletal) olivine, a screw dislocation mechanism could be still dominant for the slowly growing, flat external faces of hopper crystals. In addition, even if surface nucleation is the main growth mechanism, the limiting rate is interface diffusion and this control is enhanced with the degree of undercooling.

Likewise, evolution from skeletal to dendritic morphology reflects a change in the major growth mechanism. Formation of the dendrites is likely to involve continuous growth, which occurs concomitantly with textural ripening.

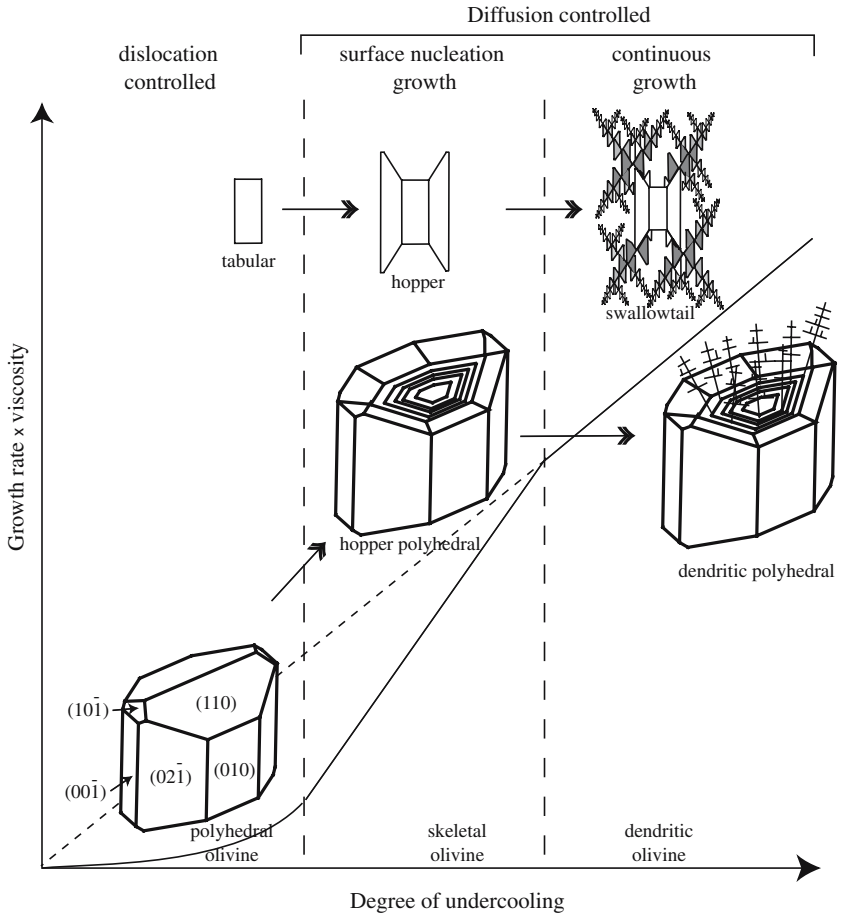

Fig. 9 Schematic diagram showing changes in olivine morphology as a function of growth mechanisms. Growth mechanisms are governed by the degree of undercooling that determines growth rates

From the petrographical point of view, two stage crystallization experiments with different cooling rates allow definition of the textural evolution of polyhedral olivine undergoing a rapid cooling episode. This evolution, namely polyhedral ⇒ hopper polyhedral ⇒ dendritic polyhedral, is similar to that for olivine grown during one stage cooling. Morphological differences within normal forsterite morphologies (polyhedral, dendrite and skeletal crystals) allow us, under certain circumstances, to decipher the complex thermal history of magmas. For instance, a recent study of complex olivine morphologies from pillow lavas of the Mid-Atlantic ridge (Faure and Schiano 2004) indicate that they reflect several cycles of cooling–heating likely to result from turbulent convection in a magmatic body. Defining the normal evolution of the morphology of polyhedral olivines is thus a potential tool for reconstructing the pre-eruptive thermal history of numerous lava flows, since it is generally believed that polyhedral crystals form at depth.

Acknowledgments We are indebted to A. Baronnet, C. Donaldson, and G. Lofgren for their careful and constructive reviews of the manuscript. The manuscript was also greatly improved by the comments of the editor J. Hoefs. We also thank J-L. Devidal for assistance with electron microprobe analyses. This is CRPG-CNRS contribution #1836.

References

Arndt NT (1994) Archean komatiites. In: Condie KC (eds) Archean crustal evolution. Elsevier, Amsterdam, pp 11–44

Baronnet A (1984) Growth kinetics of the silicates. A review of basic concepts. Fortschr Miner 62:187–232

Berg WF (1938) Crystal growth from solutions. Proc Royal Soc 164:79–95

Cabane H, Laporte D, Provost A (2005) An experimental study of Ostwald ripening of olivine and plagioclase in silicate melts: implications for the growth and size of crystals in magmas. Contrib Miner Petrol 150:37–53

Chakraborty S (1997) Rates and mechanisms of Mg–Fe interdiffusion in olivine at 980°C. J Geophys Res 102:12317–12331

Chernov AA (1974) Stability of faceted shapes. J Cryst Growth. 24/25:11–31

Deer WA, Howie RA, Zussman J (1962) Orthosilicates. Longman Group ltd, London

Devine JD, Rutherford MJ, Gardner JE (1998) Petrologic determination of ascent rate for the Soufriere Hills Volcano andesitic magma. Geophys Res Lett 25:3673–3676

Donaldson CH (1976) An experimental investigation of olivine morphology. Contrib Miner Petrol 57:187–213

Donaldson CH (1982) Spinifex-textured komatiites: a review of textures, compositions and layering. In: Arndt NT, Nisbet EG (eds) Komatiites. Allen and Unwin, London, pp 213–244

Donaldson CH, Williams RJ, Lofgren G (1975a) A sample holding technique for study of crystal growth in silicate melts. Am Miner 60:324–326

Donaldson CH, Williams TM, Lofgren GE (1975b) Experimental modeling of the cooling history of Apollo 12 olivine basalts. Proc 6th Lunar Sci Conf 843–870

Faure F, Schiano P (2004) Crystal morphologies in pillow basalts: implications for mid-ocean ridge processes. Earth Planet Sci Lett 220:331–344

Faure F, Schiano P (2005) Experimental investigation of equilibration conditions during forsterite growth and melt inclusion formation. Earth Planet Sci Lett 236:882–898

Faure F, Trolliard G, Montel JM, Nicollet C (2001) Nanopetrographic investigation of a mafic xenolith (maar de Beaunit, Massif Central, France). Eur J Miner 13:27–40

Faure F, Trolliard G, Nicollet C, Montel JM (2003a) A developmental model of olivine morphology as a function of the cooling rate and the degree of undercooling. Contrib Miner Petrol 145:251–263

Faure F, Trolliard G, Soulestin B (2003b) TEM investigation of forsterite dendrites. Am Miner 88:1241–1250

Ingrin J, Poirier JP (1986) Transmission electron microscopy of ejecta from the XVIth century eruption of the Soufriere, Guadeloupe; microscopic evidence for magma mixing. J Volcanol Geotherm Res 28:161–174

Jambon A, Lussiez P, Clocchiatti R, Weisz J, Hernandez J (1992) Olivine growth rates in a tholeiitic basalt: an experimental study of melt inclusions in plagioclase. Chem Geol 96:277–287

Kirkpatrick RJ, Kuo LC, Melchior J (1981) Crystal growth in incongruently melting compositions: programmed cooling experiments with diopside. Am Miner 66:223–241

Kossel W (1927) Zur theorie der kristallwachstums. Nachr Ges Göttingen 2:135–145

Miyamoto M, McKay DS, McKay GA, Duke MB (1986) Chemical zoning and homogenization of olivines in ordinary chondrites and implications for thermal histories of chondrules. J Geophys Res 91:12804–12816

Morgan DJ, Blake S, Rogers NW, DeVivo B, Rolandi G, Macdonald R, Hawkesworth CJ (2004) Time scales of crystal residence and magma chamber volume from modelling of diffusion profiles in phenocrysts: Vesuvius 1944. Earth Planet Sci Lett 22:933–946

Nakagawa M, Wada K, Wood CP (2002) Mixed magmas, mush chambers and eruption triggers: evidence from zoned clinopyroxene phenocrysts in andesitic scoria from the 1995 eruptions of Ruapehu Volcano, New Zealand. J Petrol 43:2279–2303

Pan Y, Batiza R (2002) Mid-ocean ridge magma chamber processes: constraints from olivine zonation in lavas from the east Pacific rise at 9°30′N and 10°30′N. J Geophys Res 107:ECV 9–1–9–13

Pyke DR, Naldrett AJ, Eckstrand OR (1973) Archean ultramafic flows in Munro Township, Ontario. Geol Soc Am Bull 84:955–978

Singer BS, Dungan MA (1995) Textures and Sr, Ba, Mg, Fe, K and Ti compositional profiles in volcanic plagioclase. Clues to the dynamics of calc-alkaline magma chambers. Am Miner 80:776–798

Stamatelopoulou-Seymour K, Vlassopoulos D, Pearce TH, Rice C (1990) The record of magma chamber processes in plagioclase phenocrysts at Thera volcano, Aegean volcanic arc, Greece. Contrib Miner Petrol 104:73–84

Stranski IN (1928) Zur theorie des kristallwachstums. Z Phys Chem 136:259–278

Sunagawa I (1981) Characteristics of crystal growth in nature as seen from the morphology of mineral crystals. Bull Minér 104:81–87

Sunagawa I (1987) Morphology of minerals. In: Sunagawa I (ed) Morphology of crystals. Terra Scientific Publishing Company, Tokyo, pp 509–587

Volmer M (1922) Crystal growth. Z Physik 9:193

Zellmer GF, Blake S, Vance D, Hawkesworth C, Turner S (1999) Plagioclase residence times at two island arc volcanoes (Kameni Islands, Santorini, and Soufriere, St Vincent) determined by Sr diffusion systematics. Contrib Miner Petrol 136:345–357